Structural Analysis of Encapsulated Single-Walled Carbon Nanotubes

D.B.Singh[1*], V.N.Shukla[2], Vikas Kumar[2], Pragya Gupta[2] and L.Ramma[3]

ABSTRACT

Tip-enhanced Raman spectroscopy revealed the nanoscale chemical properties of organic molecules encapsulated in single walled carbon nanotubes (SWNTs). Our approach is based on an enhanced electric field near a laser-irradiated metal tip functioning as a Raman excitation source. The enhanced field can successfully act on encapsulated molecules through the walls of the SWNTs to extract molecular vibrational information -carotene, which exhibits several active Raman modes under visible light illumination, was used as the encapsulated molecule. Tip-enhanced Raman spectra measured at seven different positions on SWNT bundles showed that -carotene molecules inside the tubes were not uniformly distributed. It is also found that the filling rate and peak position of the radial breathing mode of the SWNTs are linearly correlated.

Keywords: *Surface Plasmon, near-field Raman, Aperture less probe, Single- walled carbon nanotube, encapsulation*

1. INTRODUCTION

Recently, there has been a high demand for techniques for characterizing nano-composite materials. Single-walled car bon nanotubes (SWNTs) doped with organic molecules have been investigated for applications such as controlling electrical conductivity, optical switching, and nonlinear media [1–6]. Although there are many techniques for investigating and characterizing nanoscale structures, few are feasible for molecules enclosed inside nanostructures. For example, scanning tunneling microscopy (STM) has revealed spatially modulated band gap structures caused by gallium doped C82 endhedral [7]. Transmission electron microscopy (TEM) enables the visualization of molecules inside SWNTs; however, the images obtained exhibit a low contrast in the case of organic molecules [4]. Another approach is vibrational spectroscopy, including Raman spectroscopy. In comparison with that of STM, which enables the observation of electrons, vibrational energy analysis focuses is more on structural information, such as intermolecular interactions, molecular orientations, and symmetry distortions of each species. Moreover, vibrational spectroscopy can be used for identifying molecular species, which is not possible by TEM. Therefore, Raman spectroscopy is a powerful tool for studying the chemical composition of matter. Conventional confocal Raman spectroscopy techniques are limited to sub wavelength spatial resolution, and localized vibrational features of molecules encapsulated in SWNTs have not been resolved so far. This limitation has been overcome by the development of tip-enhanced Raman spectroscopy (TERS) [8–16]. By introducing a sharp metal tip to the focus of a laser beam, we were able to localize Raman excitation to an area of 30 nm^2 [17–19]. This technique has recently enabled the molecular nanoimaging of a single carbon nanotube [20] and double-stranded DNA network structures [21].

1. Dean, Department of Engineering Sciences, Global Group of Institution, Lucknow, U.P., (India)
2. Department of Engineering Sciences, Global Group of Institution, Lucknow, U.P., (India)
3. Dr. Ram Manohar Lohiya Institute of Medical Sciences, Lucknow, U.P. (India)

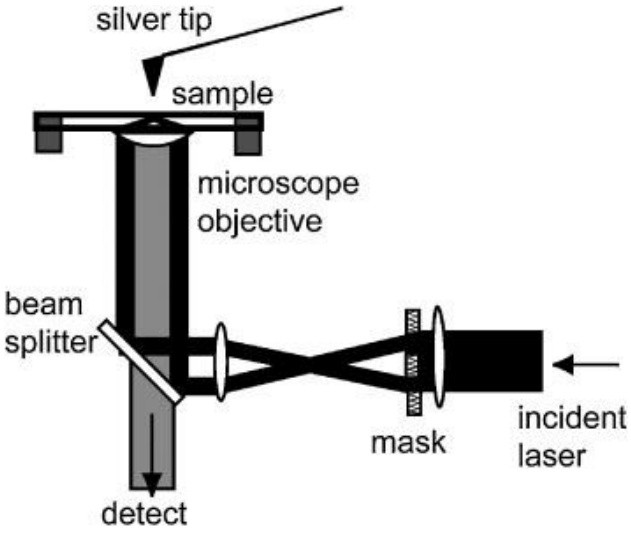

Fig. 1: Schematic diagram of TERS setup.

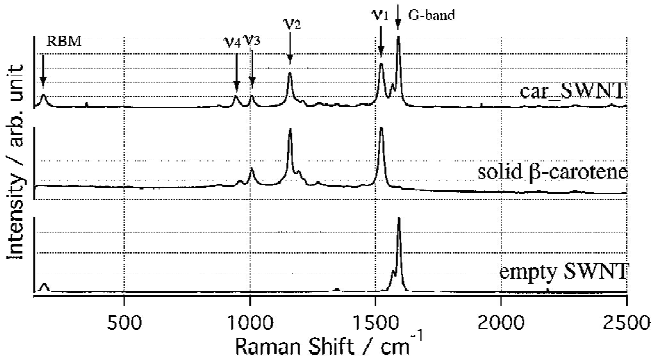

Fig. 2: Far-field Raman spectra of car SWNT, solid-carotene, and empty SWNT samples.

Preservative force to molecules, as observed by atomic force microscopy (AFM) [22].

The objective of this study is to probe the vibrational modes of organic molecules inside SWNTs. Here carotene encapsulated in SWNTs is used as samples because this molecule exhibits clear Raman peaks under visible laser excitation and is therefore suitable for further analysis.

2. EXPERIMENTAL METHODS

A schematic diagram of our apparatus is shown in Fig.1. Laser excitation was provided by a continuous-wave (CW) YAG laser (532 nm, 200 mW at the sample position). The laser intensity was set sufficiently low to avoid damage to the sample so that the exposure time does not affect near- field spectral features. Note that SWNTs are stable under near-field illumination with a laser power of up to 1 mW at 532 nm [23]. The beam was expanded 20-fold using a beam expander, and an evanescent mask was inserted in the beam path [23,24]. A cover slip, on which the sample was placed, was set on an inverted oil-immersion microscope objective lens.

The signal was guided to a single spectrometer (500 grv/mm) and detected using a liquid-nitrogen-cooled charge coupled device (CCD) camera set at an exposure time of 120 s. TERS profiles were measured using a silver tip positioned close to the sample, and reference spectra were also obtained at the same position without the silver tip. The description of experimental setup is studied [23]. The probe used as a nanolight source should be coated with noble metals to induce a surface enhanced Raman scattering (SERS) effect. Silver-coated tips were prepared by vacuum evaporation: First, a gold palladium alloy (AuPd) was deposited to a thickness of 5 nm on a silicon cantilever tip to modify the tip surface. Then, silver was evaporated to a thickness of 40 nm at a rate of 0.5 A° /s. To determine measurement position, the topography of the sample was measured. AFM images (256 x 256 pixels) were obtained in the contact mode at a scan rate of 0.4 Hz using the same silver tip as used in the TERS. SWNTs were manufactured by the laser vaporization of carbon rods doped with Co/Ni in an argon atmosphere. From the X-ray study, the average diameter of the samples ranged from 1.29 to 1.47 nm (average 1.38 nm). The method used to encapsulate -carotene inside the SWNTs is studied [6]. Briefly, -carotene (from Wako Chemicals) and SWNTs were dissolved in hexane and refluxed for 10 h in a nitrogen atmosphere. Subsequently, the solution was filtered and washed with tetrahydrofuran (THF) to produce a sheet of SWNT. The purification steps of solvent washing and filtering were repeated

three times until any - carotene that might be attached to the outside of the tube walls was removed completely. TERS, SWNTs containing encapsulated -carotene (car SWNTs) were well dispersed in THF and spin coated on a cover slip. The solvent was dried in a vacuum oven at 60^0C for 1 h. For reference, empty SWNT and solid -carotene samples were prepared. The empty SWNTs were spin-coated on a cover slip in the same manner as car SWNTs. The solid -carotene sample was prepared by dissolving it in hexane and drop-coating it onto a cover slip. The solvent was allowed to evaporate in air.

3. RESULTS AND DISCUSSION

Figure 2 shows the far-field Raman spectra of the car SWNT, solid -carotene and empty SWNT samples. The Raman shift range was set from 100 to 2500 cm 1 to investigate the correlation between the radial breathing mode (RBM) and several characteristic modes from - carotene at the same time. The observed Raman bands were assigned to the following modes: around 170 and 1592 cm 1 were attributed to RBM and the G-band of the SWNTs, respectively [25]. 1523, 1158, and 1006 cm 1 were attributed to 1 (conjugated C=C mode), 2 (C=C and C–C bond stretching mode with C–H bending), and 3 (C–CH3 stretching mode between the main chain and the side methyl carbons) of All-trans - carotene, respectively; and 944 cm 1 was attributed to 4 (out-of-plane C–H wagging), which is infrared (IR)-active [26]. In principle, the car SWNT spectrum can be reconstructed by adding the SWNT and - carotene spectra. The most significant difference was the distinct appearance of 4 at 944 cm 1 in the car SWNT spectrum, which was suppressed in the solid- carotene spectrum. This indicates that the encapsulated -carotene shows a twisted Trans conformation inside the SWNTs, otherwise, the mode is forbidden. The reason why the 4 peak appears only in the car SWNT spectrum has been discussed in ref. 6. Since this happened only in car SWNT, the 4 mode was conveniently used as a marker band for encapsulation. The objective of our investigation is to probe -carotene inside SWNTs with a nanometer spatial resolution. Figures 3(a) and 3(b) show AFM images of the car SWNT samples. We chose two different bundles that were completely separated. The crosses (a to g) indicate the position of the tip during the TERS, which was performed in 100 nm steps along the bundles. From the AFM image, the heights of the bundles were found to be on average 16 nm as shown in Fig. 3(a) and 12 nm as shown in Fig. 3(b). These indicate that these bundles consisted of collections of several tens of tubes. Near-field Raman spectra are shown in Figs. 4(a) to 4(c). Near-field spectra here mean the difference between the spectra with the silver tip in contact with the sample and the spectra without the tip. Spectra a to g correspond to the sample positions in Fig. 3. Figure 4(a) shows the high-frequency region including both 1and the G-band. The most predominant feature among the spectra 'a to g' is the absence of encapsulated - carotene in spectrum f. This means that the local filling rate of the car SWNTs was not uniform. The extremely low filling rate at the position could have occurred when the tubes were wrenched during encapsulation or were filled with impurities. Another feature is that in spectrum c, the

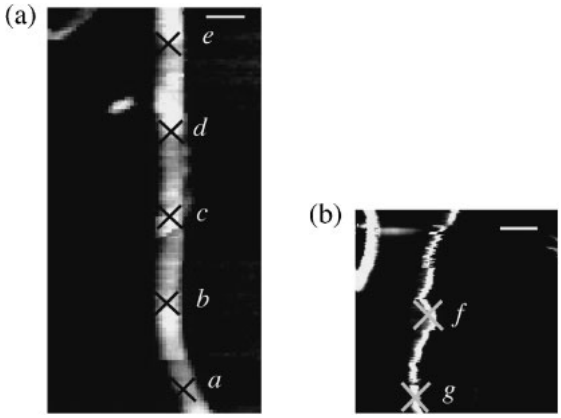

Fig. 3: AFM images of car SWNT bundles measured. Crosses indicate the selected positions of the tip during TERS measurement: (a) a to e, and (b) f and g. The scale bar is 50 nm.

Intensity of encapsulated - carotene is higher than compared with other spectra. Figure 3(a) shows the presence of another thin bundle entangled with a thicker one. For simplicity, we assume that the amplitude ratio of the SWNTs to encapsulate - carotene is proportional to the number of encapsulated molecules in the SWNTs. From Lorenzian curve-fitting parameters, the amplitude ratios I 1 =IG are 1.63, 1.50, 1.99, 1.81, 1.51, 0, and 1.34 for spectra a to g, respectively. This tip site dependence of I 1 =IG suggests that the -carotene was encapsulated

in homogeneously inside the SWNTs. The intermediate region is shown in Fig. 4(b). In this figure, the 4 mode appears in all the spectra, except spectrum f . As we mentioned earlier, this peak is evidence of the twisted conformation of the encapsulated - carotene. This result suggests that the - carotene molecules prevented the twisted conformation to occur in all observation points; no other conformation was found. Figure 4(c) shows the low-frequency region of the car SWNTs, which involves RBM. The peak position of RBM is inversely proportional to the tube diameter of the SWNTs, as expressed by the formula[25].

$$W_R = 246/d$$

Where W_R and d are the peak position of RBM and the diameter of the corresponding tube, respectively. Applying Lorenzian curve fitting to spectra a to g, !R values were determined to be 182.5, 182.2, 177.9, 179.1, 181.5, 184.1, and 183.7 cm 1 , respectively. Since our samples were bundles of tubes, d here is the average tube diameter. It has been reported that when molecules are encapsulated in SWNTs, the RBM band becomes lower and broad.4) Note that spectrum f, which is free of encapsulated molecules, exhibits a fairly sharp spectral feature. To assess the relationship of tube diameter and local filling rate, the RBM Raman shift and I 1 =IG was plotted, as shown in Fig. 5.

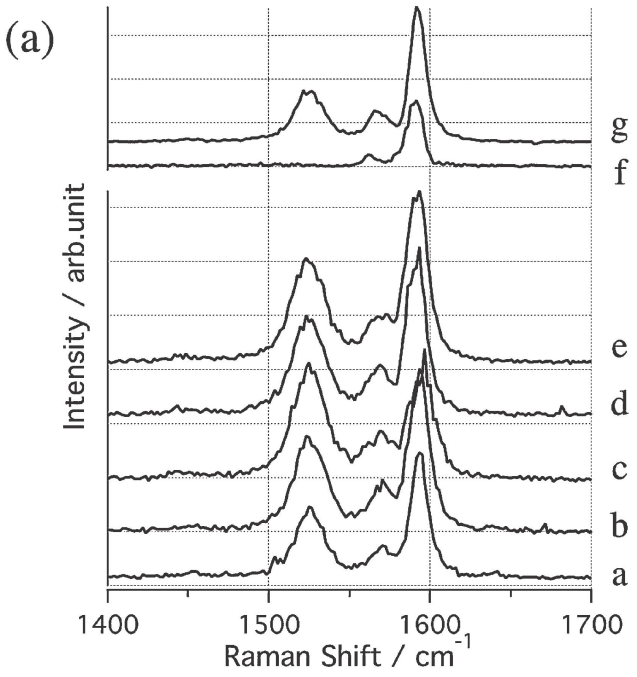

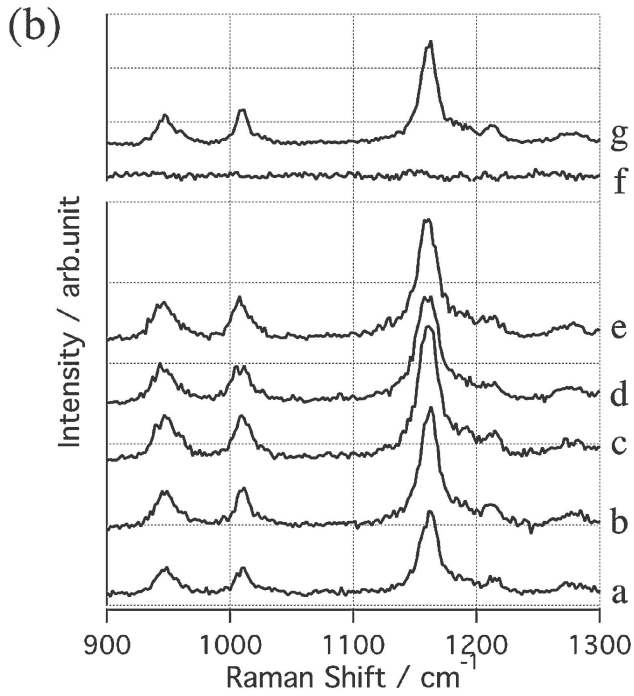

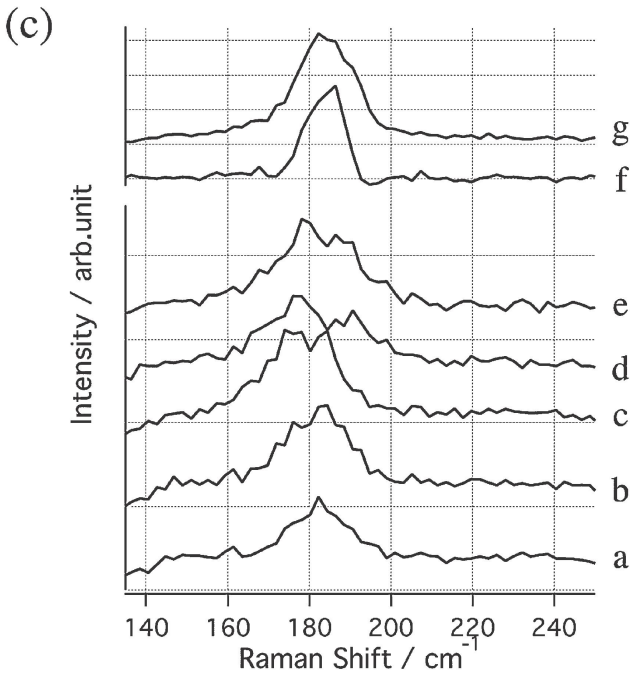

Fig. 4: Near-field Raman spectra of car SWNTs. Curves a to g correspond to the spectra measured at the positions shown in Fig. 3. Each spectrum is displayed with an offset for clarity. (a) High-frequency, (b) intermediate- frequency, and (c) low-frequency ranges.

S-JPSET : ISSN : 2229-7111, Vol. 2, Issue 2

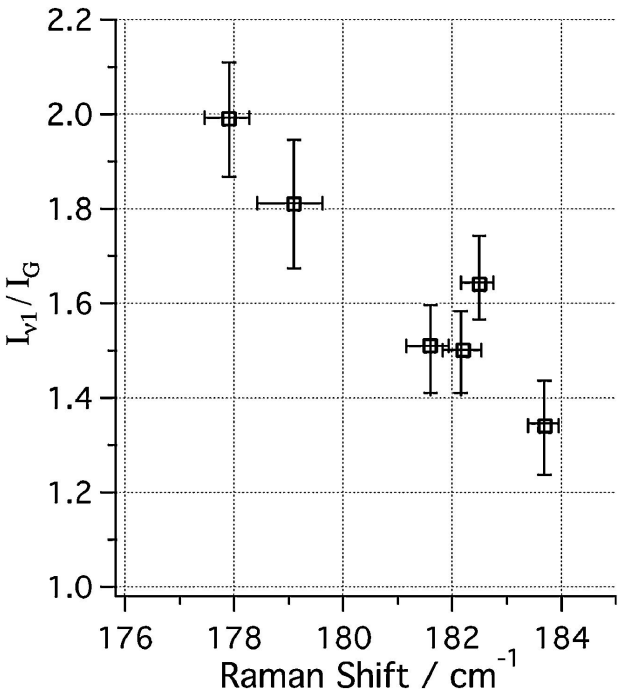

Fig. 5: Correlation between peak position of RBM and local filling rates of -carotene at positions a to g (except f) in Fig. 3. Fitting errors are shown.

The curve-fitting procedures was applied for determining values, and the fitting errors are shown on the graph. Filling rate (I 1 =IG) and the RBM Raman shift are linearly correlated. Assuming that eq. (1) holds, the tubes with larger diameters show a smaller Raman shift. Therefore, Fig. 5 shows that larger tubes exhibit higher filling rates. This conclusion is supported by the report that larger tubes are energetically preferable for encapsulating diacety- lene chains[27].The smallest tube diameter for encapsulation, which is determined by the size and affinity between tubes and molecules, has been investigated [28]. Here, any lower or upper limit of the diameter could not be found for encapsulation. From Fig. 5, the filling rate is depend on tube diameter since I 1 =IG varied from 1.2 to 2.0, although tube diameter differed by only 3%. These findings suggest the possibility of a lower or upper limit of tube diameter for encapsulation when the distribution of tube diameters is broader.

4. CONCLUSIONS

From the above study, the molecular vibrational information of -carotene encapsulated was found sucessful in SWNTs by TERS. The principle of this method is to use tip-enhancement, which provides both spectral information and topological information at the same time; this method can be applied not only to surfaces but also to molecules enclosed inside nanostructures. The results showed the nanoscale inhomogeneity of the sample. Local filling rates was estimated at seven different positions on the SWNT bundles from the intensity ratio I 1=IG of 1 and the G-band. Furthermore, the relationship between the peak position of RBM and the filling rate suggests that thicker tubes are preferable for encapsulation. This work demonstrates that TERS spectroscopy is useful for avoiding the averaging of Raman spectra of nano-composite materials that are not spatially uniform.

REFERENCES

[1] H. Kataura, Y. Maniwa, T. Kodama, K. Kikuchi, K. Hirahara, K. Suenaga, S. Iijima, S. Suzuki, Y. Achiba and W. Kra¨tschmer: Synth. Met. 121 (2001) 1195.

[2] L. J. Li, A. N. Khlobystov, J. G. Wiltshire, G. A. D. Briggs and R. J. Nicholas: Nat. Mater. 4 (2005) 481.

[3] B. W. Smith, M. Monthioux and D. E. Luzzi: Nature 396 (1998) 323.

[4] T. Takenobu, T. Takano, M. Shiraishi, Y. Murakami, M. Ata, H. Kataura, Y. Achiba and Y. Iwasa: Nat. Mater. 2 (2003) 683.

[5] F. Simon, H. Kuzmany, H. Rauf, T. Pichler, J. Bernardi, H. Peterlik, L. Korecz, F. Fu¨ lo¨ p and A. Ja´nossy: Chem. Phys. Lett. 383 (2004) 362.

[6] K. Yanagi, Y. Miyata and H. Kataura: Adv. Mater. 18 (2006) 437.

[7] J. Lee, H. Kim, S.-J. Kahng, G. Kim, Y.-W. Son, J. Ihm, H. Kato, Z. W. Wang, T. Okazaki, H. Shinohara and Y. Kuk: Nature 415 (2002)

[8] Y. Inouye, N. Hayazawa, K. Hayashi, Z. Sekkat and S. Kawata: Proc. SPIE 3791 (1999) 40.

[9] N. Hayazawa, Y. Inouye, Z. Sekkat and S. Kawata: Opt. Commun. 183 (2000) 333.

[10] M. S. Anderson: Appl. Phys. Lett. 76 (2000) 3130.

[11] R. M. Sto¨ ckle, Y. D. Suh, V. Deckert and R. Zenobi: Chem. Phys Lett. 318 (2000) 131.

[12] N. Hayazawa, Y. Inouye, Z. Sekkat and S. Kawata: Chem. Phys. Lett. 335 (2001) 369.

[13] J. J. Wang, D. A. Smith, D. N. Batchelder, Y. Saito, J. Kirkham, C. Robinson, K. Baldwin, G. Li and B. Bennett: J. Microsc. 210 (2002) 330.

[14] D. S. Bulgarevich and M. Futamata: Appl. Spectrosc. 58 (2004) 757.

[15] B. Pettinger, B. Ren, G. Picardi, R. Schuster and G. Ertl: Phys. Rev. Lett. 92 (2004) 096101.

[16] N. Hayazawa, T. Yano, H. Watanabe, Y. Inouye and S. Kawata: Chem. Phys. Lett. 376 (2003) 174.

[17] Y. Inouye and S. Kawata: Opt. Lett. 19 (1994) 159.

[18] A. Lahrech, R. Bachelot, P. Gleyzes and A. C. Boccara: Opt. Lett. 21 (1996) 1315.

[19] B. Knoll and F. Keilmann: Nature 399 (1999) 134.

[20] A. Hartschuh, E. J. Sa´nchez, X. S. Xie and L. Novotny: Phys. Rev. Lett. 90 (2003) 095503.

[21] T. Ichimura, N. Hayazawa, M. Hashimoto, Y. Inouye and S. Kawata: Appl. Phys. Lett. 84 (2004) 1768.

[22] T. Yano, Y. Inouye and S. Kawata: Nano Lett. 6 (2006) 1269.

[23] Y. Saito, N. Hayazawa, H. Kataura, T. Murakami, K. Tsukagoshi, Y. Inouye and S. Kawata: Chem. Phys. Lett. 410 (2005) 136.

[24] N. Hayazawa, Y. Inouye and S. Kawata: J. Microsc. 194 (1999) 472.

[25] R. Saito, G. Dresselhous and M. S. Dresselhous: Physical Properties of Carbon Nanotubes (Imperial College Press, London, 1998).

[26] B. Robert: in The Photochemistry of Cartenoids, ed. H. A. Frank, A. J. Young, G. Britton and R. J. Cogdell (Kluwer Academic, Dordrecht, 1999) Chap. 10.

[27] G. C. McIntosh, D. Toma´nek and Y. W. Park: Phys. Rev. B 67 (2003) 125419.

[28] S. Bandow, M. Takizawa, H. Kato, T. Okazaki, H. Shinohara and S. Iijima: Chem. Phys. Lett. 347 (2001) 23.

